

FediOS: Decoupling Orthogonal Subspaces for Personalization in Feature-skew Federated Learning

Lingzhi Gao^{1*} Zexi Li^{1*} Yang Lu² Chao Wu^{1†}
¹Zhejiang University ²Xiamen University

{lingzhigao, zexi.li, chao.wu}@zju.edu.cn luyang@xmu.edu.cn

Abstract

Personalized federated learning (pFL) enables collaborative training among multiple clients to enhance the capability of customized local models. In pFL, clients may have heterogeneous (also known as non-IID) data, which poses a key challenge in how to decouple the data knowledge into generic knowledge for global sharing and personalized knowledge for preserving local personalization. A typical way of pFL focuses on label distribution skew, and they adopt a decoupling scheme where the model is split into a common feature extractor and two prediction heads (generic and personalized). However, such a decoupling scheme cannot solve the essential problem of feature skew heterogeneity, because a common feature extractor cannot decouple the generic and personalized features. Therefore, in this paper, we rethink the architecture decoupling design for feature-skew pFL and propose an effective pFL method called FediOS. In FediOS, we reformulate the decoupling into two feature extractors (generic and personalized) and one shared prediction head. Orthogonal projections are used for clients to map the generic features into one common subspace and scatter the personalized features into different subspaces to achieve decoupling for them. In addition, a shared prediction head is trained to balance the importance of generic and personalized features during inference. Extensive experiments on four vision datasets demonstrate our method reaches state-of-the-art pFL performances under feature skew heterogeneity.

1. Introduction

Federated learning (FL) [17, 25, 32, 37] is a distributed machine learning paradigm that enables collaborative training among multiple clients under the coordination of a central server. Unlike centralized learning, FL does not collect client data, therefore preserving data privacy and owner-

*Equal contributions.

†Corresponding author.

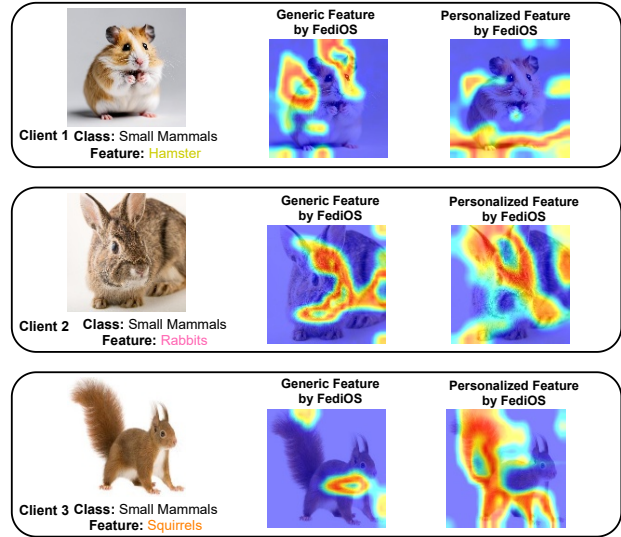


Figure 1. **Feature visualization of the proposed FediOS.** Three clients with the same class (small mammals) but different feature spaces (**hamster**, **rabbits**, and **squirrels**). It is found that FediOS can effectively decouple generic and personalized features. According to small mammals, FediOS extracts the common **generic features** on the faces (mouths/eyes) and fur (color/texture). For the **personalized features**, they are decoupled as follows: **hamster**—the small and pink feet; **rabbits**—the big ears; **squirrels**—the furry tail and the relatively long feet.

ship [25, 32], also, it is communication-efficient [4, 32].

In FL, personalized federated learning (pFL) aims to improve the capability of clients’ customized models through federated training [3, 19, 23, 37]. pFL addresses the concerns about why the clients need to join FL training (i.e., motivation) and what can they get from the FL training (i.e., incentive and credit). It has wide applications in computer vision, such as image classification [3, 33], image segmentation [9, 41], and medical images [5, 49]. However, data heterogeneity is a key challenge in pFL, because different clients may have diverse preferences and user behaviors and, as a result, generate data that are non-IID with each

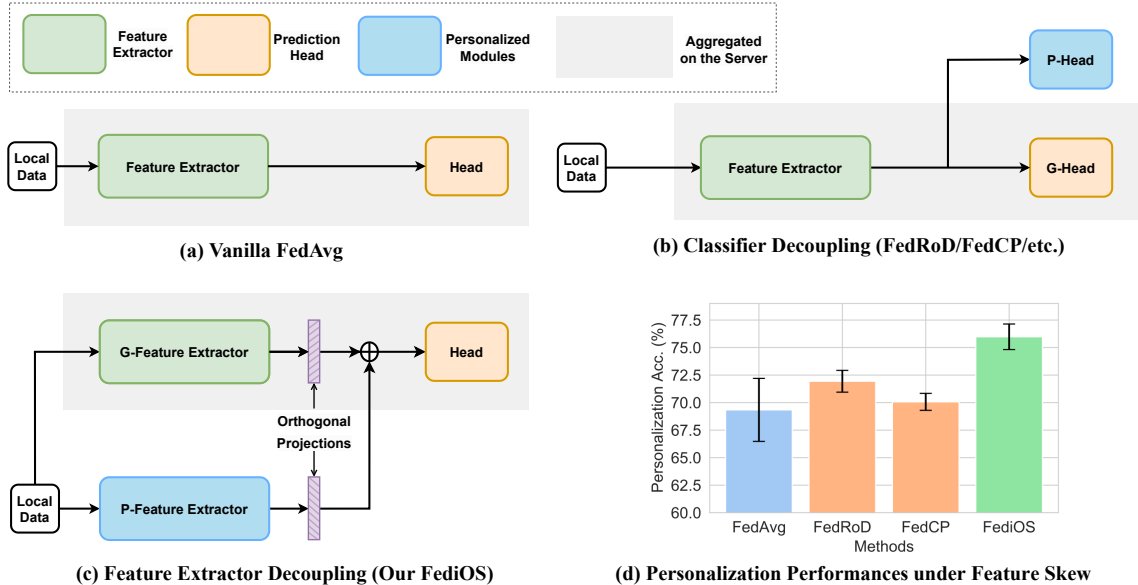


Figure 2. **Comparison of architecture decoupling designs.** (a) Vanilla FedAvg without decoupling. (b) Previous pFL methods decouple the prediction heads which may be ineffective under feature skew. (c) Our proposed FediOS decouples feature extractors through orthogonal subspaces. (d) Personalization performances under feature skew (Office-Caltech-10 with 4 clients). It is shown that prediction-head-decoupled methods have marginal improvements over FedAvg while our feature-extractor-decoupled FediOS have significant results.

other [21, 40]. For learning and optimization, data heterogeneity means that clients have diverse learning objectives that are *partially in common but partially inconsistent*. To realize better personalization, a fundamental research question is posted:

How to decouple the data knowledge into generic knowledge for global sharing and personalized knowledge for preserving local personalization?

To answer the question, we need to understand how data heterogeneity emerges in practice. Mainly, there are two types of data heterogeneity: (a) **label distribution skew** [3, 21, 22, 47] which is described as the heterogeneity of $\mathcal{P}(y)$ among clients and (b) **feature skew** [15, 30, 51] which refers to the heterogeneity of $\mathcal{P}(x)$ or $\mathcal{P}(x|y)$, where x denotes the feature of data and y is the label¹. Label distribution skew and feature skew are both common in practice. Take the photo classification as an example, some phone users may like dogs more than cats, so they have more dog photos (label distribution skew); for dog lovers, according to the same label of “dog”, someone’s dog is a Shiba while another user has a Husky, and different breeds of dogs have different visual features (feature skew).

Most previous works of pFL focus on label distribution skew [3, 6, 22, 48]. To decouple the generic and personalized knowledge, they adopt a decoupling scheme where the model is split into a common feature extractor and two

prediction heads (generic and personalized) [3, 16, 44, 48] since the imbalance in labels will result in more drifts in the heads (e.g., for the classification task, the classifiers). The prediction-head-decoupled architecture is shown in Figure 2 (b). However, for feature skew heterogeneity, one common feature extractor cannot suit all clients with divergent feature spaces, and decoupling the heads cannot address the problem since the generic and personalized features are encoded by the feature extractors, not the heads. In Figure 2 (d), it is revealed that the methods of decoupling the heads have marginal improvements over vanilla FedAvg under feature skew. Therefore, rethinking the architecture decoupling design in feature-skew pFL is urgently needed.

In this paper, we reckon *instead of decoupling the heads, we need to decouple the feature extractors for feature-skew pFL*. But how to effectively and efficiently decouple the features? Inspired by the orthogonal projections in continual learning, we propose **Federated learning with decoupling Orthogonal Subspaces (FediOS)**. In FediOS, as illustrated in Figure 2 (c), orthogonal projections are used for clients to map the generic features into one common subspace and scatter the personalized features into different subspaces. All clients share identical generic projections, whereas their personalized projections are mutually orthogonal and also orthogonal to the generic projections. We also devise a loss to regularize and strengthen the orthogonality. In addition, a shared prediction head is trained to balance the importance of generic and personalized features during inference.

By leveraging the orthogonal subspaces, our FediOS can

¹Besides, in some less common cases such as clustered FL, heterogeneity of $\mathcal{P}(y|x)$ is also considered [11, 24, 36].

effectively decouple generic and personalized features, and an intuitive example is presented in Figure 1. In the figure, for the class of small mammals, FediOS extracts common features as generic features such as faces (mouths/eyes) and fur (color/texture), meanwhile, it also decouples the diverse personalized features such as furry tails for squirrels and big ears for rabbits. Additionally, from Figure 2 (d), it is obvious that compared with previous decoupling schemes, FediOS can improve the personalization performances by a large margin under feature skew heterogeneity. We also note that the orthogonal projections in FediOS are set-and-fixed and learning-free, which is much more efficient than some feature disentanglement techniques that require training additional variational autoencoders (VAEs) [8, 31].

To sum up, our contributions are as follows.

- We rethink the architecture decoupling design in feature-skew pFL and propose to decouple feature extractors instead of classifiers.
- We propose FediOS, which uses orthogonal projections to decouple generic and personalized features under the structure of dual feature extractors.
- Extensive experiments on four vision datasets, Office-Caltech-10, DomainNet, Digits-Five, and CIFAR-100, validate that our FediOS reaches state-of-the-art personalization performances under feature skew. Interestingly, it can also improve the generalization by effective generic knowledge sharing through decoupling.

2. Related Work

Federated Learning. Since FedAvg [32] is first proposed, many federated learning methods are then designed to tackle data heterogeneity among clients for better generalization [1, 21], personalization [19, 37], robustness [22, 42, 43], fairness [22, 46], and efficiency [4, 12]. Besides personalization, the generalization of the global model is a key goal for FL training. It is deemed that better generalization of global models is the foundation of better personalization of local models [3, 27]. To achieve better generalization, algorithms tackling data heterogeneity from the perspectives of server-side aggregation and client-side local updates are both needed. For server aggregation, ensemble distillation [28] and improved weighted aggregation [26, 45] are proposed; while for client updates, techniques like proximal descent [21], dynamic regularization [1], normalized gradients [40], and classifier calibration [27, 29] are tailored for resolving non-IID data, especially label distribution skew. For feature skew, a prototypical method based on prototype clustering is proposed to improve the generalization [15].

Personalized Federated Learning. Personalized federated learning aims to improve the customized capability of clients’ local models on the personalized local datasets [19, 37]. Most of the previous works in pFL improve personalization under **label distribution skew**: Architecture de-

coupling is first proposed in FedRep [6] to boost personalization. In FedRep, the feature extractor and the prediction head are decoupled and the server only aggregates the feature extractors while keeping the heads to be local and personalized. Afterward, FedRoD [3] further strengthens the decoupling design, as presented in Figure 2 (b), it is proposed to have two prediction heads, one for generalization (G-Head) with balanced empirical loss and another one for personalization (P-Head) with vanilla loss. FedRoD aggregates the feature extractor and the G-Head and keeps the P-Head local. Following the prediction-head-decoupled scheme in Figure 2 (b), FedTHE [16] balances the prediction weights of two heads for test-time robust personalization, and FedCP [48] uses conditional policy to determine the proportion of global and local information within the two heads. Despite of its success in label skew, in this paper, we argue that the prediction-head-decoupled methods may not be effective enough under feature skew. Apart from decoupling, other methods are developed to improve personalization under label skew. FedBABU [33] proposes to fix the parameters of the head during the training process and only needs to fine-tune it locally at the end. FedNH [7] improves personalization through prototypes, that it uses the smoothing-averaged prototypes as the classification heads.

For **feature-skew personalization**, FedBN [23] keeps the Batch Normalization layers of each client model locally and uploads other parts of the model for aggregation to solve the impact of domain shift between clients. pFed-VEM [51] is a framework that estimates uncertainty and model deviation among clients to derive a confidence value. This value then regulates the classifier head’s weight during aggregation, facilitating the identification of common patterns and minimizing model discrepancies. In AlignFed [50], the model on each client is separated into a personalized feature extractor and a shared classifier and collaboration is conducted by sharing and aggregating feature prototypes. By aggregating heads instead of feature extractors, it is the first attempt to rethink the decoupling under feature skew. But AlignFed does not go further into the decoupling that it cannot effectively decouple generic and personalized features by using one personalized feature extractor. It is notable that our method has a novel decoupling scheme compared with previous algorithms and it is shown to be effective and efficient in decoupling generic and personalized features.

3. Method

3.1. Learning Objectives

Basic Settings. We introduce a typical FL setting with N clients holding potentially feature-skew heterogeneous data partitions $\mathcal{D}_1, \dots, \mathcal{D}_N$, respectively. For one data sample, we use x to notate the data features and y to denote the

labels. The feature-skew heterogeneity among clients is defined as the following formulation:

$$\mathcal{P}_i(x|y) \neq \mathcal{P}_j(x|y), \forall i, j \in [N], i \neq j, \quad (1)$$

where $\mathcal{P}_i(x|y)$ is the conditional probability of x given y for client i . The whole training data is the sum of all local data as $\mathcal{D} \triangleq \bigcup_i^N \mathcal{D}_i$.

The model architecture Θ contains two parts, a feature extractor parameterized by W and a prediction head parameterized by H , i.e., $\Theta = \{W, H\}$. The clients collaboratively train the models with data locally kept under the coordination of a central server.

Generalization Objective. The global objective is to collaboratively train a generalized global model, which can be represented as:

$$\min_{\Theta} \mathcal{L}(\Theta) = \sum_{i=1}^N \frac{|\mathcal{D}_i|}{|\mathcal{D}|} \mathcal{L}_i(\Theta), \quad (2)$$

where $|\mathcal{D}|$ is the number of data samples and $\mathcal{L}_i(\Theta)$ denotes the empirical risk of client i as following:

$$\mathcal{L}_i(\Theta) = \sum_{k=1}^{|\mathcal{D}_i|} \frac{1}{|\mathcal{D}_i|} l(y_k, f(x_k; \Theta)), \quad (3)$$

where $(x_k, y_k) \in \mathcal{D}_i$ is the data of client i , $f(\cdot; \cdot)$ is the model function that generates outputs given the parameters, and $l(\cdot, \cdot)$ is the loss function that measures the difference between the outputs of the model and the truth labels.

Personalization Objective. In pFL, every client aims to have their own personalized models that can perform better personalization on their own datasets. The learning objective of pFL is:

$$\min_{\{\Theta_1, \dots, \Theta_N\} \in \Theta} \mathcal{L}(\Theta) = \sum_{i=1}^N \frac{|\mathcal{D}_i|}{|\mathcal{D}|} \mathcal{L}_i(\Theta_i), \quad (4)$$

where Θ_i denotes the personalized model parameters for client i . Finally, we will get a set of personalized models $\Theta^* = \{\Theta_1^*, \dots, \Theta_N^*\}$ to better adapt to clients' local data distributions.

We note that the generalization and the personalization objectives are not conflicted. As discussed in the literature, great generalization is the foundation of great personalization performances [3, 27]. Also, in this paper, we discover how to decouple the generic/generalized representation knowledge from clients to enhance local personalization better under feature-skew heterogeneity.

3.2. Decoupling Orthogonal Feature Subspaces

Instead of decoupling the heads, for feature-skew heterogeneity, we propose to decouple the feature extractor into

two, one for generic feature extraction and another for personalized features. *But how to realize such an effective decoupling?* A straightforward way is resorting to feature disentanglement techniques that are commonly used in feature debiasing [8, 31]. However, disentanglement techniques usually require training an additional VAE, which is computation-expensive at edge clients. Thus, to enable efficient and effective decoupling, we adopt the orthogonal subspace technique, which was previously used in continual learning for solving the catastrophic forgetting problem [2]. Compared with the VAE methods, the orthogonal subspace method [2] is set-and-fixed and learning-free, and it is highly effective in solving our problem. We first give the definition of orthogonal subspace as follows.

Definition 3.1 (Orthogonal Subspace). The vector space S has two subspaces S_1 and S_2 . S_1 and S_2 are said to be orthogonal if any vectors in each subspace are pair-wisely orthogonal, written as:

$$\mathbf{v}_1 \cdot \mathbf{v}_2 = 0, \quad \forall \mathbf{v}_1 \in S_1, \mathbf{v}_2 \in S_2. \quad (5)$$

Orthogonal projections facilitate orthogonal feature subspaces. In continual learning, orthogonal projections are used to enable the time-varying data to be learned into different subspaces of one model [2]. Inspired by this, in our work, we use orthogonal projections to learn orthogonal feature representations of two different feature extractors, i.e., the generic and personalized.

We use the projection matrices that satisfy the following orthogonal and normalized properties:

$$P_i^\top P_i = I; P_i^\top P_j = 0, i \neq j. \quad (6)$$

Given the raw data feature x , we assume the feature extractor W produces the extracted feature as $\phi_W = f(x; W)$. After applying a projection matrix P_i , the extracted feature is $\phi_{P_i} = P_i \phi_W$. We will show that by applying orthogonal projections P_i and P_j that satisfy Equation (6), we can have orthogonal gradient updates, as a result, obtaining the orthogonal model parameters and feature spaces.

Assuming that each feature extractor consists of L hidden layers, an input sample x will be passed in each layer as follows: the l -th layer's output is $h_l = \sigma(h_{l-1}; W_l)$, where $\sigma(\cdot)$ is an activation function, W_l is the parameter of the l -th layer, $h_0 = x$, and $h_L = \phi_W$. Therefore, $\phi_{P_i} = P_i h_L$. In the training process, for any projection matrix P_i , the gradient of any intermediate layer h_l can be decomposed into:

$$\begin{aligned} g_l^{P_i} &= \frac{\partial l}{\partial h_l} = \left(\frac{\partial l}{\partial h_L} \right) \frac{\partial h_L}{\partial h_l} = \left(\frac{\partial \phi_{P_i}}{\partial h_L} \frac{\partial l}{\partial \phi_{P_i}} \right) \frac{\partial h_L}{\partial h_l} \\ &= \left(P_i \frac{\partial l}{\partial \phi_{P_i}} \right) \prod_{k=l}^{L-1} \frac{\partial h_{k+1}}{\partial h_k} = g_L^{P_i} \prod_{k=l}^{L-1} D_{k+1} W_{k+1}, \quad (7) \end{aligned}$$

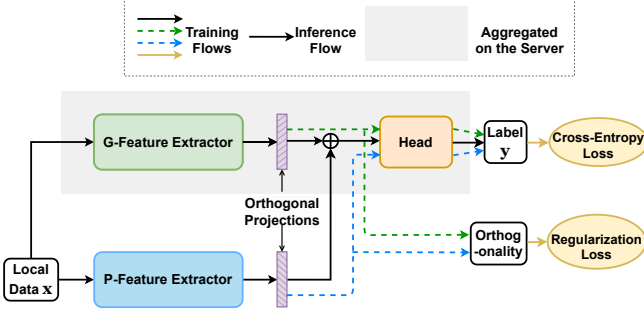


Figure 3. Training and inference illustrations of FediOS.

where D_{k+1} is the Jacobian matrix and we assume it to be an identity. It can be seen that for any layer in the feature extractor, its gradient is associated with the last layer’s gradient $g_L^{P_i}$; and for orthogonal projections $P_i \perp P_j$, the last layer’s gradients are orthogonal that $g_L^{P_i} \perp g_L^{P_j}$. Due to the orthogonal gradient updates, we can have orthogonal model parameters and feature spaces.

As shown in Figure 3, for each client $i \in [N]$, we have a generic feature extractor (parameterized by W_i^g), a personalized feature extractor (parameterized by W_i^p) with the same structure, and one prediction head (parameterized by H_i). All clients have the same generic projection P^g for the generic feature extractor and have distinct personalized projections P_i^p , $\forall i \in [N]$ for their personalized extractors. All the projections $\mathbf{P} = \{P^g, P_1^p, \dots, P_N^p\}$, including one generic and N personalized, are synthesized at initialization and fixed during training, and they satisfy the orthogonal and normalized properties in Equation (6) pair-wisely. This ensures that all the generic feature extractors are learned in a common subspace and all the personalized extractors are orthogonal with each other and are also orthogonal with the generic extractor.

3.3. Training Stage

For each client i , $\forall i \in [N]$, given a data sample $(x_k, y_k) \in \mathcal{D}_i$, the generic feature $\phi_{i,k}^g$ and the personalized feature $\phi_{i,k}^p$ are given by:

$$\phi_{i,k}^g = P^g f(x_k; W_i^g), \phi_{i,k}^p = P_i^p f(x_k; W_i^p). \quad (8)$$

We also have a fused feature representation $\phi_{i,k}^f$:

$$\phi_{i,k}^f = \alpha \phi_{i,k}^g + (1 - \alpha) \phi_{i,k}^p, \quad (9)$$

where α is the hyperparameter controlling the proportion of the generic feature. Generally, α is set around 0.5 to have a balance between the generic and personalized features. Interestingly, we will show in the experimental part (Figure 5), that different datasets may have slightly different

optimal α , indicating the intrinsic generic-or-personalized feature structures of the datasets.

The Cross-Entropy Loss. During the training process, we employ the cross-entropy loss function to optimize the model parameters. By using one common prediction head H_i , we compute the cross-entropy loss for the three features $\phi_{i,k}^f, \phi_{i,k}^g, \phi_{i,k}^p$, respectively.

$$\mathcal{L}_{ce} = - \frac{1}{|\mathcal{D}_i|} \left(\underbrace{\sum_{k=1}^{|\mathcal{D}_i|} y_k \log(f(\phi_{i,k}^f; H_i))}_{\text{fused features}} + \underbrace{\sum_{k=1}^{|\mathcal{D}_i|} y_k \log(f(\phi_{i,k}^g; H_i))}_{\text{generic features}} + \underbrace{\sum_{k=1}^{|\mathcal{D}_i|} y_k \log(f(\phi_{i,k}^p; H_i))}_{\text{personalized features}} \right). \quad (10)$$

In this way, the prediction head is learned to balance the tradeoff between the generic and the personalized features, and the two feature extractors are both trained to effectively contribute to the personalization task.

The Orthogonality Regularization Loss. Additionally, we utilize the absolute value of the inner product between generic and personalized features as a loss function to strengthen the orthogonality between these two features:

$$\mathcal{L}_{re} = \frac{1}{|\mathcal{D}_i|} \sum_{k=1}^{|\mathcal{D}_i|} |\phi_{i,k}^g \cdot \phi_{i,k}^p|. \quad (11)$$

Finally, the overall loss function is:

$$\mathcal{L} = \mathcal{L}_{ce} + \lambda \mathcal{L}_{re}, \quad (12)$$

where λ is the hyper-parameter to control the strength of the regularization loss. The clients conduct Equation (12) for E epochs and communicate with the server.

Server-side Aggregation. After the client i completes local training, the generic feature extractor W_i^g and the prediction head H_i will be uploaded to the server and aggregated by FedAvg [32]. The overall number of communication and local training rounds is T . The training procedure is shown in Figure 3 and Algorithm 1 in the appendix.

3.4. Inference Stage

During the personalization inference stage on the client side, we only use the fused features defined in Equation (9), and the learned prediction head can implicitly balance the tradeoff between the generic and personalized features. The inference workflow is also illustrated in Figure 3. To validate the global model on the server, we use only the aggregated generic feature extractor, the generic projection, and the aggregated prediction head.

Table 1. **Results in terms of personalization accuracy (%) of local models on four datasets under different numbers of clients (N).** The best methods in each setting are highlighted in **bold** fonts.

Dataset	Office-Caltech-10		DomainNet		Digits-Five		CIFAR-100	
Number of Clients (N)	4	12	6	12	5	10	5	10
Local	70.67±1.56	46.71±1.31	38.34±1.69	30.45±0.82	85.41±0.57	79.17±0.24	62.06±0.74	49.20±4.71
FedAvg ₂₀₁₇ [32]	69.34±2.86	55.47±1.54	36.40±3.35	29.50±1.22	86.78±0.74	86.46±0.72	54.87±1.58	52.81±0.13
FedDyn ₂₀₂₁ [1]	69.57±1.96	56.03±0.25	39.47±3.23	26.98±2.39	84.80±0.14	84.97±0.35	45.45±0.41	43.07±1.76
MOON ₂₀₂₁ [20]	63.15±6.56	52.74±5.60	35.02±2.89	27.45±0.64	84.16±0.11	78.92±0.97	52.40±0.37	50.20±0.41
Ditto ₂₀₂₁ [22]	72.04±0.40	53.63±0.59	43.13±0.89	33.83±0.50	81.77±0.38	72.98±0.16	58.25±0.61	45.88±4.27
FedProto ₂₀₂₂ [39]	70.32±1.53	49.25±1.07	40.17±1.23	31.04±0.65	87.23±0.28	82.41±0.05	60.27±0.40	50.01±3.85
FedRoD ₂₀₂₂ [3]	71.94±0.99	57.45±2.04	40.50±3.06	32.40±3.19	86.39±0.23	86.72±0.12	58.87±0.76	56.27±0.82
FedCP ₂₀₂₃ [48]	70.07±0.77	52.16±0.78	41.36±1.19	29.51±1.38	87.28±0.09	86.48±0.09	54.21±0.46	53.96±0.72
FedBN ₂₀₂₁ [23]	71.75±1.31	59.70±0.22	41.64±3.41	36.79±1.02	87.17±0.54	86.82±0.57	54.87±0.58	52.81±0.13
pFedVEM ₂₀₂₃ [51]	70.32±2.58	58.86±2.47	39.85±2.50	27.56±1.19	81.28±1.05	80.11±0.71	55.08±0.50	51.15±1.69
Our FediOS	75.98±1.16	60.60±0.80	45.90±0.37	37.32±0.43	88.65±0.49	86.94±0.10	64.99±0.72	58.00±2.17

4. Experiment

4.1. Experimental Settings

Datasets and Models. Following previous works [23, 30, 50, 51], we use four vision datasets to simulate feature-skew heterogeneity in FL: Office-Caltech-10 [10], DomainNet [34], Digits-Five [34], and CIFAR-100 [18]. **(1) Feature skew with domain shifts.** Office-Caltech-10 (4 domains), DomainNet (6 domains), and Digits-Five (5 domains) are the datasets that contain domain shifts. By using these datasets in FL, clients have heterogeneous datasets with feature-skew domain shifts [23, 50]. **(2) Natural feature skew with different subclasses.** CIFAR-100 contains 20 superclasses and each superclass contains 5 subclasses. It is found that within each superclass, images from different subclasses have natural feature skew, where common feature patterns and distinct/personalized features may both exist. Following previous work [51], we use the superclasses as the prediction labels and craft natural feature skew by assigning different subclasses to clients. For the models, if not mentioned otherwise, we use ResNet18 [13] for Office-Caltech-10 and DomainNet, a six-layer CNN [23] for Digits-Five, and a four-layer CNN [48] for CIFAR-100. Due to space limits, for more data and model details, please refer to the appendix.

Compared Methods. We use 5 sets of 9 FL algorithms as baselines that are strong or are most relevant to our method. **(1) Vanilla FedAvg.** FedAvg [32] is the first FL algorithm but is also shown to be a strong baseline in pFL scenarios [3]. **(2) Generalized FL methods.** Generalization is the foundation of personalization, therefore, we compare the state-of-the-art FL methods targeting generalization and see how they perform under feature-skew personalization. It includes FedDyn [1], FL with dynamic regularization; MOON [20], FL with model contrastive learning. **(3) General pFL methods.** We compare two common and

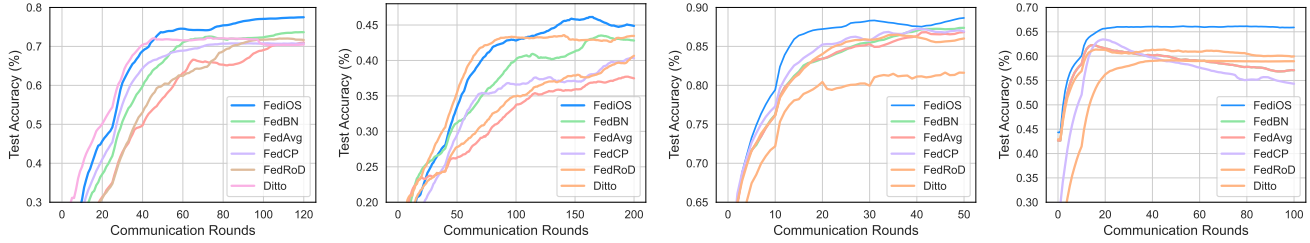
strong pFL methods, which are Ditto [22], personalization by using global models to regularize local model training; FedProto [39], personalization by using prototypes to extract information from a class-based perspective. **(4) Prediction-head-decoupled pFL methods.** We compare the pFL methods decoupling the prediction heads, which are shown to be state-of-the-art in label distribution skew [3, 48]. FedRoD [3], pFL method using balanced and personalized losses respectively in two heads. FedCP [48], separating feature information via conditional policy in two heads. **(5) pFL methods tailored for feature skew.** We also validate previous feature-skew pFL methods. FedBN [23], personalization by retaining the Batch Normalization layer. pFedVEM [51], the state-of-the-art feature-skew pFL method with adjusting aggregation via variational expectation maximization.

Client Settings. We set the number of clients N to be a multiple of the number of domains or superclasses, and each client only has one domain/superclass’s data. Specifically, $N \in \{4, 12\}$ for Office-Caltech-10, $N \in \{6, 12\}$ for DomainNet, $N \in \{5, 10\}$ for Digits-Five, and $N \in \{5, 10\}$ for CIFAR-100. In each round, we test the local models after training [3] on clients’ local test datasets and take the average accuracy of clients as the personalization performance [3, 48]. We record the personalized performance in each round and take the average of the last 5 rounds as the result. The settings of E and T are in the appendix.

Implementation. In all experiments, we conduct experiments under three different seeds and present the mean accuracy and the standard deviation.

4.2. Main Results

Results under various vision datasets. Table 1 shows the personalization performance of different methods under various datasets. We can find that our method achieves state-of-the-art performances in all settings. Meanwhile,



(a) Office-Caltech-10 with $N = 4$. (b) DomainNet with $N = 6$. (c) Digits-Five with $N = 5$. (d) CIFAR-100 with $N = 5$.

Figure 4. Personalization test accuracy curves of the methods under various datasets.

Table 2. Results in terms of generalization accuracy (%) of global models.

Dataset	Digits-Five		CIFAR-100	
	5	10	5	10
FedAvg [32]	83.89±0.51	83.45±0.29	49.00±0.20	48.38±0.74
Ditto [22]	84.15±0.27	83.45±0.18	48.42±0.06	48.65±0.73
FedRoD [3]	83.80±0.10	83.41±0.18	48.55±0.52	48.44±0.43
FedCP [48]	83.87±0.13	82.86±0.27	41.63±0.52	42.79±0.31
pFedVEM [51]	77.94±1.02	78.52±0.34	42.73±0.66	44.16±0.46
Our FediOS	84.47±0.19	83.85±0.25	49.05±0.24	48.83±0.30

we visualize the training curves of the model in Figure 4. We can find that our method can achieve higher accuracy and converge more smoothly and quickly. As the number of clients increases, the local data for each client will decrease. In this case, we find that for traditional pFL methods, like FedProto and Ditto, which keep personalized models local, their performances will be significantly affected. For prediction-head-decoupled methods like FedRoD and FedCP, they usually can get better results than FedAvg, but the gains are marginal. This is because, in feature-skew heterogeneity, knowledge mainly comes from the feature extractors, and the dual classifier heads cannot achieve effective knowledge decoupling. While our FediOS uses a dual-feature-extractor decoupling, and in most cases, it reaches state-of-the-art results. The effectiveness of FediOS’s feature decoupling is visualized in Figure 1, where generic features are extracted and generic knowledge is shared.

Results regarding generalization. Although our method is designed to improve personalization, interestingly, we find that by effectively decoupling and sharing the generic knowledge, the generalization of the global models can also be improved for FediOS. We test the global models after aggregation on a test dataset with all domains/subclasses to indicate the generalization. In Table 2, we show the generalization accuracies of different methods. It is found that our FediOS can still achieve a leading performance among the pFL baselines.

Results under different N with partial client sampling. Scalability is an essential issue for FL methods [21], and when the number of clients N increases, due to the communication budget, it is needed to implement partial client sampling instead of full participation. In CIFAR-100, we increase the number of clients and experiment with differ-

Table 3. Results (%) under various numbers of clients with partial client sampling. The dataset is CIFAR-100.

Number of Clients	15		20	
	0.6	1.0	0.6	1.0
Methods/Sampling rate				
FedAvg [32]	52.18±0.51	51.75±0.61	45.40±1.53	46.80±1.00
FedCP [48]	54.22±0.17	53.14±0.37	47.54±2.84	47.60±1.99
FedRoD [3]	54.51±0.06	54.82±0.65	49.89±0.87	49.40±1.50
pFedVEM [51]	49.32±0.74	49.80±0.04	48.64±1.21	48.45±0.82
Our FediOS	54.93±0.31	55.59±0.37	51.51±2.10	50.95±2.41

Table 4. Results (%) under different local epochs (E). The dataset is Digits-Five with $N = 5$.

Methods/ E	2	3	5	10
FedAvg [32]	86.55±0.13	86.62±0.51	86.49±0.23	86.41±0.19
FedBN [23]	86.27±0.15	86.83±0.29	86.47±0.19	86.34±0.35
FedCP [48]	86.96±0.41	86.77±0.17	86.65±0.24	86.59±0.31
FedRoD [3]	86.52±0.48	86.22±0.16	86.40±0.25	86.14±0.34
Our FediOS	88.29±0.16	88.40±0.05	87.69±0.18	87.39±0.45

ent client sampling rates. In each round of communication, we randomly select a set of clients for model aggregation according to the sampling rate and then send the aggregated model to all clients. In Table 3, we can find that our method still performs well among various baselines.

Results under different local epochs E . Larger number of local epochs E results in fewer required communication round T , achieving more communication-efficient FL training. We conduct experiments with larger E . In Table 4, we find that as E increases, the accuracies of most methods decrease, but our FediOS also maintains the best results.

Results regarding more model architectures. We verify the effectiveness of our FediOS by using more model architectures, i.e., ResNet18 [13], EfficientNet [38], MobileNetV2 [35], and DenseNet121 [14]. Compared with the previously used four-layer CNN model, these neural networks have more complex structures and contain more parameters. As Table 6 indicates, our FediOS can improve personalization in various neural network architectures, which verifies the rationale of our decoupling scheme and the effectiveness of the orthogonal projections. At the same time, we find that as the complexity of the network structure increases, the advantage of FedRoD and FedBN diminishes as it has closer results with FedAvg, whereas our method still has notable performance gains.

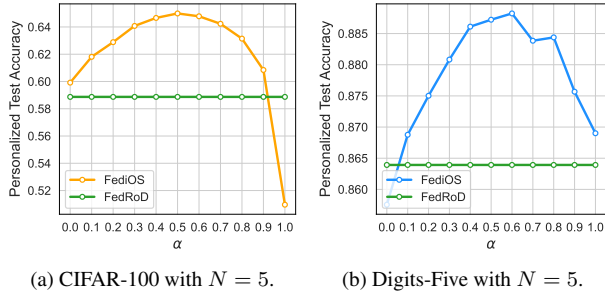


Figure 5. Results of FediOS under different α .

Table 5. Results (%) of our FediOS using different λ . The dataset is Office-Caltech-10 with $N = 4$.

λ	0.1	1.0	10.0	50.0
Our FediOS	75.98±1.16	76.07±0.75	75.04±1.61	71.87±0.99

4.3. Sensitivity Analysis of Hyperparameters

Our FediOS introduces additional hyperparameters λ and α , and we will present their sensitivity analyses.

Analysis of the hyperparameter α . In FediOS, α controls the proportion of the generic feature when fusing features, and it also reveals the balance between the generic and personalized knowledge. In our implementation, we generally keep $\alpha = 0.5$ to keep the uniform balance. While in Figure 5, we make a sensitivity analysis of α to see the optimal values of α under different datasets. Generally, α has a wide range of values to be superior to FedRoD, so FediOS is not sensitive to α . It has the optimal values around 0.5; for CIFAR-100, the optimal value is 0.5, and for Digits-Five, the value is 0.6. A higher optimal value of α for Digits-Five means that it benefits more on the generic knowledge sharing. The visualization of case samples in each dataset is in the appendix. It is intuitively reasonable that digital numbers share more common and simpler patterns across domains compared with CIFAR-100, therefore, Digits-Five is prone to have higher weights of the generic feature. Intriguingly, it reveals that the intrinsic generic-or-personalized feature structures of the datasets can be explicitly explored by the optimal α of FediOS.

Analysis of the hyperparameter λ . In FediOS, the hyperparameter λ is for controlling the strength of the orthogonal regularization loss. We set λ to different values to explore its impact on the algorithm performance. The larger the value of λ , the more attention the model will pay to the orthogonality of generic features and personalized features. As Table 5 shows, we observe an optimization-regularization tradeoff regarding different λ . When λ is small and appropriate, it can further strengthen the orthogonality of generic and personalized features, thus, improving personalization. However, if λ is too large, the orthogonality regularization will limit the optimization of learning effective representations, and it will even cause negative ef-

Table 6. Results (%) of our FediOS using different model architectures. The dataset is CIFAR-100 with $N = 5$.

Model	FedAvg	FedBN	FedRoD	FediOS
ResNet18 [13]	64.59±0.37	65.32±0.46	65.28±0.23	69.21±0.49
EfficientNet [38]	68.45±0.71	68.99±0.58	69.28±0.58	73.70±0.75
MobileNetV2 [35]	73.88±0.47	73.34±0.33	73.89±0.38	76.76±0.18
DenseNet121 [14]	83.79±0.37	83.43±0.36	83.75±0.92	86.19±0.46

Table 7. Ablation study of FediOS in terms of personalization. The datasets are Office-Caltech-10 with $N = 4$ and DomainNet with $N = 12$.

Dataset	Office-Caltech-10	DomainNet
FedAvg	69.34±2.86	29.50±1.22
Ours w/o Orthogonal Projections	71.77±0.90	26.64±1.92
Ours w/o Personalized Extractors	72.29±1.00	30.48±1.43
Ours w/o \mathcal{L}_{re}	75.43±0.97	36.32±0.86
Ours	75.98±1.16	37.32±0.43

fects. We suggest to keep λ small and around 1 to have a mild and appropriate regularization. We also find that λ is not sensitive if being kept small.

4.4. Ablation Study

We conduct the ablation study of FediOS’s modules in Table 7. It is found that each part of our approach plays an important role, and they work together to achieve better performance. Notably, we notice that orthogonal projection has the most vital impact on the improvement. If without orthogonal projections, the performance shows a huge drop-off, even lower than FedAvg in some cases. This suggests that only using two feature extractors cannot effectively decouple the knowledge, and the orthogonal projections are quite essential. We also find that when FediOS is only without the personalized feature extractor, the model still performs slightly better than FedAvg. It reveals that the projection matrix may map the model parameters into a subspace where the knowledge is more aligned, so it will surpass vanilla FedAvg. Moreover, \mathcal{L}_{re} plays the role of strengthening the orthogonality of generic and personalized features, helping to achieve better results.

5. Conclusion

In this paper, we rethink the architecture decoupling design in feature-skew personalized federated learning and propose FediOS. Specifically, for each client, We set up a shared generic feature extractor and a local personalized feature extractor. FediOS uses orthogonal projections to map the generic features into one common subspace and scatter the personalized features into different subspaces to achieve feature decoupling. As validated by extensive experiments, our method achieves state-of-the-art feature-skew personalization results compared to strong baselines and can also improve generalization. Furthermore, we gained insights into the effectiveness and applicability of our approach.

References

- [1] Durmus Alp Emre Acar, Yue Zhao, Ramon Matas, Matthew Mattina, Paul Whatmough, and Venkatesh Saligrama. Federated learning based on dynamic regularization. In *International Conference on Learning Representations*, 2020. 3, 6
- [2] Arslan Chaudhry, Naemullah Khan, Puneet Dokania, and Philip Torr. Continual learning in low-rank orthogonal subspaces. *Advances in Neural Information Processing Systems*, 33:9900–9911, 2020. 4
- [3] Hong-You Chen and Wei-Lun Chao. On bridging generic and personalized federated learning for image classification. In *International Conference on Learning Representations*, 2022. 1, 2, 3, 4, 6, 7
- [4] Mingzhe Chen, Nir Shlezinger, H Vincent Poor, Yonina C Eldar, and Shuguang Cui. Communication-efficient federated learning. *Proceedings of the National Academy of Sciences*, 118(17):e2024789118, 2021. 1, 3
- [5] Zhen Chen, Meilu Zhu, Chen Yang, and Yixuan Yuan. Personalized retrogress-resilient framework for real-world medical federated learning. In *Medical Image Computing and Computer Assisted Intervention—MICCAI 2021: 24th International Conference, Strasbourg, France, September 27–October 1, 2021, Proceedings, Part III 24*, pages 347–356. Springer, 2021. 1
- [6] Liam Collins, Hamed Hassani, Aryan Mokhtari, and Sanjay Shakkottai. Exploiting shared representations for personalized federated learning. In *International conference on machine learning*, pages 2089–2099. PMLR, 2021. 2, 3
- [7] Yutong Dai, Zeyuan Chen, Junnan Li, Shelby Heinecke, Lichao Sun, and Ran Xu. Tackling data heterogeneity in federated learning with class prototypes. In *Proceedings of the AAAI Conference on Artificial Intelligence*, pages 7314–7322, 2023. 3
- [8] Zheng Ding, Yifan Xu, Weijian Xu, Gaurav Parmar, Yang Yang, Max Welling, and Zhuowen Tu. Guided variational autoencoder for disentanglement learning. In *Proceedings of the IEEE/CVF conference on computer vision and pattern recognition*, pages 7920–7929, 2020. 3, 4
- [9] Jiahua Dong, Duzhen Zhang, Yang Cong, Wei Cong, Henghui Ding, and Dengxin Dai. Federated incremental semantic segmentation. In *Proceedings of the IEEE/CVF Conference on Computer Vision and Pattern Recognition*, pages 3934–3943, 2023. 1
- [10] Basura Fernando, Amaury Habrard, Marc Sebban, and Tinne Tuytelaars. Subspace alignment for domain adaptation. *arXiv preprint arXiv:1409.5241*, 2014. 6, 11
- [11] Avishek Ghosh, Jichan Chung, Dong Yin, and Kannan Ramchandran. An efficient framework for clustered federated learning. *Advances in Neural Information Processing Systems*, 33:19586–19597, 2020. 2
- [12] Jenny Hamer, Mehryar Mohri, and Ananda Theertha Suresh. Fedboost: A communication-efficient algorithm for federated learning. In *International Conference on Machine Learning*, pages 3973–3983. PMLR, 2020. 3
- [13] Kaiming He, Xiangyu Zhang, Shaoqing Ren, and Jian Sun. Deep residual learning for image recognition. In *Proceedings of the IEEE conference on computer vision and pattern recognition*, pages 770–778, 2016. 6, 7, 8
- [14] Gao Huang, Zhuang Liu, Laurens van der Maaten, and Kilian Q. Weinberger. Densely connected convolutional networks. In *Proceedings of the IEEE Conference on Computer Vision and Pattern Recognition (CVPR)*, 2017. 7, 8
- [15] Wenke Huang, Mang Ye, Zekun Shi, He Li, and Bo Du. Rethinking federated learning with domain shift: A prototype view. In *CVPR*, 2023. 2, 3
- [16] Liangze Jiang and Tao Lin. Test-time robust personalization for federated learning. *arXiv preprint arXiv:2205.10920*, 2022. 2, 3
- [17] Peter Kairouz, H Brendan McMahan, Brendan Avent, Aurélien Bellet, Mehdi Bennis, Arjun Nitin Bhagoji, Kallista Bonawitz, Zachary Charles, Graham Cormode, Rachel Cummings, et al. Advances and open problems in federated learning. *Foundations and Trends® in Machine Learning*, 14(1–2):1–210, 2021. 1
- [18] Alex Krizhevsky, Geoffrey Hinton, et al. Learning multiple layers of features from tiny images. 2009. 6, 11
- [19] Viraj Kulkarni, Milind Kulkarni, and Aniruddha Pant. Survey of personalization techniques for federated learning. In *2020 Fourth World Conference on Smart Trends in Systems, Security and Sustainability (WorldS4)*, pages 794–797. IEEE, 2020. 1, 3
- [20] Qinbin Li, Bingsheng He, and Dawn Song. Model-contrastive federated learning. In *Proceedings of the IEEE/CVF conference on computer vision and pattern recognition*, pages 10713–10722, 2021. 6
- [21] Tian Li, Anit Kumar Sahu, Manzil Zaheer, Maziar Sanjabi, Ameet Talwalkar, and Virginia Smith. Federated optimization in heterogeneous networks. *Proceedings of Machine Learning and Systems*, 2:429–450, 2020. 2, 3, 7
- [22] Tian Li, Shengyuan Hu, Ahmad Beirami, and Virginia Smith. Ditto: Fair and robust federated learning through personalization. In *International Conference on Machine Learning*, pages 6357–6368. PMLR, 2021. 2, 3, 6, 7
- [23] Xiaoxiao Li, Meirui JIANG, Xiaofei Zhang, Michael Kamp, and Qi Dou. Fedbn: Federated learning on non-iid features via local batch normalization. In *International Conference on Learning Representations*, 2021. 1, 3, 6, 7, 11, 12
- [24] Zexi Li, Jiaxun Lu, Shuang Luo, Didi Zhu, Yunfeng Shao, Yinchuan Li, Zhimeng Zhang, Yongheng Wang, and Chao Wu. Towards effective clustered federated learning: A peer-to-peer framework with adaptive neighbor matching. *IEEE Transactions on Big Data*, 2022. 2
- [25] Zexi Li, Feng Mao, and Chao Wu. Can we share models if sharing data is not an option? *Patterns*, 3(11):100603, 2022. 1
- [26] Zexi Li, Tao Lin, Xinyi Shang, and Chao Wu. Revisiting weighted aggregation in federated learning with neural networks. In *Proceedings of the 40th International Conference on Machine Learning*, pages 19767–19788. PMLR, 2023. 3
- [27] Zexi Li, Xinyi Shang, Rui He, Tao Lin, and Chao Wu. No fear of classifier biases: Neural collapse inspired federated learning with synthetic and fixed classifier. In *Proceedings of the IEEE/CVF International Conference on Computer Vision (ICCV)*, pages 5319–5329, 2023. 3, 4

- [28] Tao Lin, Lingjing Kong, Sebastian U Stich, and Martin Jaggi. Ensemble distillation for robust model fusion in federated learning. *Advances in Neural Information Processing Systems*, 33:2351–2363, 2020. [3](#)
- [29] Mi Luo, Fei Chen, Dapeng Hu, Yifan Zhang, Jian Liang, and Jiashi Feng. No fear of heterogeneity: Classifier calibration for federated learning with non-iid data. *Advances in Neural Information Processing Systems*, 34:5972–5984, 2021. [3](#)
- [30] Zhengquan Luo, Yunlong Wang, Zilei Wang, Zhenan Sun, and Tieniu Tan. Disentangled federated learning for tackling attributes skew via invariant aggregation and diversity transferring. In *International Conference on Machine Learning*, pages 14527–14541. PMLR, 2022. [2](#), [6](#)
- [31] Emile Mathieu, Tom Rainforth, Nana Siddharth, and Yee Whye Teh. Disentangling disentanglement in variational autoencoders. In *International conference on machine learning*, pages 4402–4412. PMLR, 2019. [3](#), [4](#)
- [32] Brendan McMahan, Eider Moore, Daniel Ramage, Seth Hampson, and Blaise Aguera y Arcas. Communication-efficient learning of deep networks from decentralized data. In *Artificial intelligence and statistics*, pages 1273–1282. PMLR, 2017. [1](#), [3](#), [5](#), [6](#), [7](#)
- [33] Jaehoon Oh, SangMook Kim, and Se-Young Yun. Fedbabu: Toward enhanced representation for federated image classification. In *International Conference on Learning Representations*, 2022. [1](#), [3](#)
- [34] Xingchao Peng, Qinxun Bai, Xide Xia, Zijun Huang, Kate Saenko, and Bo Wang. Moment matching for multi-source domain adaptation. In *Proceedings of the IEEE/CVF international conference on computer vision*, pages 1406–1415, 2019. [6](#), [11](#)
- [35] Mark Sandler, Andrew Howard, Menglong Zhu, Andrey Zhmoginov, and Liang-Chieh Chen. Mobilenetv2: Inverted residuals and linear bottlenecks. In *Proceedings of the IEEE Conference on Computer Vision and Pattern Recognition (CVPR)*, 2018. [7](#), [8](#)
- [36] Felix Sattler, Klaus-Robert Müller, and Wojciech Samek. Clustered federated learning: Model-agnostic distributed multitask optimization under privacy constraints. *IEEE transactions on neural networks and learning systems*, 32(8):3710–3722, 2020. [2](#)
- [37] Alysia Ziyang Tan, Han Yu, Lizhen Cui, and Qiang Yang. Towards personalized federated learning. *IEEE Transactions on Neural Networks and Learning Systems*, 2022. [1](#), [3](#)
- [38] Mingxing Tan and Quoc Le. Efficientnet: Rethinking model scaling for convolutional neural networks. In *International conference on machine learning*, pages 6105–6114. PMLR, 2019. [7](#), [8](#)
- [39] Yue Tan, Guodong Long, Lu Liu, Tianyi Zhou, Qinghua Lu, Jing Jiang, and Chengqi Zhang. Fedproto: Federated prototype learning across heterogeneous clients. In *Proceedings of the AAAI Conference on Artificial Intelligence*, pages 8432–8440, 2022. [6](#), [12](#)
- [40] Jianyu Wang, Qinghua Liu, Hao Liang, Gauri Joshi, and H Vincent Poor. Tackling the objective inconsistency problem in heterogeneous federated optimization. *Advances in neural information processing systems*, 33:7611–7623, 2020. [2](#), [3](#)
- [41] Jiacheng Wang, Yueming Jin, Danail Stoyanov, and Liansheng Wang. Feddp: Dual personalization in federated medical image segmentation. *IEEE Transactions on Medical Imaging*, 2023. [1](#)
- [42] Chenrui Wu, Zexi Li, Fangxin Wang, and Chao Wu. Learning cautiously in federated learning with noisy and heterogeneous clients. In *2023 IEEE International Conference on Multimedia and Expo (ICME)*, pages 660–665, Los Alamitos, CA, USA, 2023. IEEE Computer Society. [3](#)
- [43] Jingyi Xu, Zihan Chen, Tony QS Quek, and Kai Fong Ernest Chong. Fedcorr: Multi-stage federated learning for label noise correction. In *Proceedings of the IEEE/CVF Conference on Computer Vision and Pattern Recognition*, pages 10184–10193, 2022. [3](#)
- [44] Jian Xu, Xinyi Tong, and Shao-Lun Huang. Personalized federated learning with feature alignment and classifier collaboration. In *The Eleventh International Conference on Learning Representations*, 2022. [2](#)
- [45] Rui Ye, Mingkai Xu, Jianyu Wang, Chenxin Xu, Siheng Chen, and Yanfeng Wang. Feddisco: Federated learning with discrepancy-aware collaboration. In *Proceedings of the 40th International Conference on Machine Learning*, pages 39879–39902. PMLR, 2023. [3](#)
- [46] Fengda Zhang, Kun Kuang, Yuxuan Liu, Long Chen, Chao Wu, Fei Wu, Jiayun Lu, Yunfeng Shao, and Jun Xiao. Unified group fairness on federated learning. *arXiv preprint arXiv:2111.04986*, 2021. [3](#)
- [47] Jie Zhang, Zhiqi Li, Bo Li, Jianghe Xu, Shuang Wu, Shouhong Ding, and Chao Wu. Federated learning with label distribution skew via logits calibration. In *International Conference on Machine Learning*, pages 26311–26329. PMLR, 2022. [2](#)
- [48] Jianqing Zhang, Yang Hua, Hao Wang, Tao Song, Zhengui Xue, Ruhui Ma, and Haibing Guan. Fedcp: Separating feature information for personalized federated learning via conditional policy. In *Proceedings of the 29th ACM SIGKDD Conference on Knowledge Discovery and Data Mining*, pages 3249–3261, 2023. [2](#), [3](#), [6](#), [7](#), [11](#), [12](#)
- [49] Ruipeng Zhang, Ziqing Fan, Qinwei Xu, Jiangchao Yao, Ya Zhang, and Yanfeng Wang. Grace: A generalized and personalized federated learning method for medical imaging. In *International Conference on Medical Image Computing and Computer-Assisted Intervention*, pages 14–24. Springer, 2023. [1](#)
- [50] Guogang Zhu, Xuefeng Liu, Shaojie Tang, and Jianwei Niu. Aligning before aggregating: Enabling cross-domain federated learning via consistent feature extraction. In *2022 IEEE 42nd International Conference on Distributed Computing Systems (ICDCS)*, pages 809–819. IEEE, 2022. [3](#), [6](#)
- [51] Junyi Zhu, Xingchen Ma, and Matthew B Blaschko. Confidence-aware personalized federated learning via variational expectation maximization. In *Proceedings of the IEEE/CVF Conference on Computer Vision and Pattern Recognition*, pages 24542–24551, 2023. [2](#), [3](#), [6](#), [7](#), [12](#)

Appendix

A. Pseudo Code of FediOS

In Algorithm 1, we show the detailed training stage of our approach. In the training process, each client i will simultaneously train a global feature extractor W_i^g and prediction head H_i received from the server, as well as a personalized feature extractor W_i^p that remains local, guided by the loss function \mathcal{L} in Equation (12) of the main paper.

Algorithm 1 FediOS Training Stage

Input: N clients with local data \mathcal{D} , communication round T , local epoch E , local learning rate η , projection layers $\mathbf{P} = \{P^g, P_1^p, \dots, P_N^p\}$;

Parameter: initial generic feature extractor W^g , initial personalized feature extractor W^p , initial classifier head H , and hyperparameters α, λ ;

Output: a final generic feature extractor, N final personalized feature extractors, and a final classifier head;

- 1: Server sends projection layers and initial models to client $i, \forall i \in [N]$.
 - 2: **for** each round $t = 1, \dots, T$ **do**
 - 3: # Client updates
 - 4: **for** each client $i, i \in [N]$ **in parallel do**
 - 5: set $W_i^{g,t} \leftarrow W^{g,t-1}, W_i^{p,t} \leftarrow W_i^{p,t-1}, H_i^t \leftarrow H^{t-1}$;
 - 6: **for** each epoch $e = 1, \dots, E$ **do**
 - 7: **for** $(x_k, y_k) \in \mathcal{D}_i$ **do**
 - 8: $\phi_{i,k}^g \leftarrow (x_k; W_i^g, P^g)$ in Eq. (8),
 - 9: $\phi_{i,k}^p \leftarrow (x_k; W_i^p, P_i^p)$ in Eq. (8),
 - 10: $\phi_{i,k}^f \leftarrow \alpha \phi_{i,k}^g + (1 - \alpha) \phi_{i,k}^p$;
 - 11: Compute loss \mathcal{L} by Eq. (12);
 - 12: $W_i^{g,t} \leftarrow W_i^{g,t} - \eta \nabla \mathcal{L}$;
 - 13: $W_i^{p,t} \leftarrow W_i^{p,t} - \eta \nabla \mathcal{L}$;
 - 14: $H_i^t \leftarrow H_i^t - \eta \nabla \mathcal{L}$;
 - 15: **end for**
 - 16: **end for**
 - 17: **end for**
 - 18: # Server aggregation
 - 19: $W^{g,t+1} = \sum_{i \in N} \frac{|\mathcal{D}_i|}{|\mathcal{D}|} W_i^{g,t}$;
 - 20: $H^{t+1} = \sum_{i \in N} \frac{|\mathcal{D}_i|}{|\mathcal{D}|} H_i^t$;
 - 21: **end for**
 - 22: **return** Obtain global model $W^{g,T}, H^T$ and personalized feature extractor $W_i^{p,T}$ for client $i, \forall i \in [N]$.
-

B. Experimental Details

B.1. Datasets

Office-Caltech-10 [10]. Office-Caltech-10 has four data sources: the Amazon merchant website, the Caltech-101 dataset, a high-resolution DSLR camera, and a webcam. Each source represents a domain, and each domain has the same 10 classes for classification tasks.

DomainNet [34]. DomainNet is a dataset containing images from six domains. Each domain represents a style, namely Clipart, Infograph, Painting, Quickdraw, Real, and Sketch. The DomainNet contains 345 object categories, following [23], we choose the top ten most common classes for our experiments.

Digits-Five [34]. Digits-Five is a combination of five digits recognition datasets: MNIST, MNIST-M, Synthetic Digits, SVHN, and USPS. Each dataset represents a style and is divided into ten categories from digits 0 to 9.

CIFAR-100 [18]. Each image in CIFAR-100 has two labels: superclass and subclass. Each subclass can be included in a superclass. There are 500 training images and 100 testing images per subclass. CIFAR-100 has 20 superclasses and each superclass has 5 subclasses. The images from different subclasses within each superclass share some common features. For example, for the superclass of flowers, there are five subclasses, namely, orchid, poppy, rose, sunflower, and tulip.

Visualization. To give a more intuitive demonstration of the feature-skew datasets, in Figure 6, we visualize some cases of samples from each dataset.

B.2. Model Architectures

For Office-Caltech-10 and DomainNet, we use ResNet-18 and the implementation code refers to [48]. For Digits-Five, we use a six-layer CNN that referred from [23]. For CIFAR-100, we use a four-layer CNN that referred from [48]. We show the details of the network structure in Table 8 and Table 9. For the convolutional layer (Conv2D), the parameters we present are input and output dimension, kernel size, stride, and padding. For the max pooling layer (MaxPool2D), we present kernel and stride. For the Batch Normalization layer (BN), we present the channel dimension. For the fully connected layer (FC), we present the input and output dimensions. In the paper, we use the last fully connected layer of the network as the prediction head and the rest as the feature extractor.

Table 8. **Model architectures of six-layer CNN [23] for Digit-Five.**

Layer	Details
1	Conv2D(3, 64, 5, 1, 2), BN(64), ReLU, MaxPool2D(2,2)
2	Conv2D(64, 64, 5, 1, 2), BN(64), ReLU, MaxPool2D(2,2)
3	Conv2D(64, 128, 5, 1, 2), BN(128), ReLU
4	FC(6272,2048), BN(2048), ReLU
5	FC(2048,512), BN(512), ReLU
6 (Head)	FC(512,10)

Table 9. **Model architectures of four-layer CNN [48] for CIFAR-100.**

Layer	Details
1	Conv2D(3, 32, 5, 0, 1), ReLU, MaxPool2D(2,2)
2	Conv2D(32, 64, 5, 1, 2), ReLU, MaxPool2D(2,2)
3	FC(1600,512), ReLU
4 (Head)	FC(512,20)

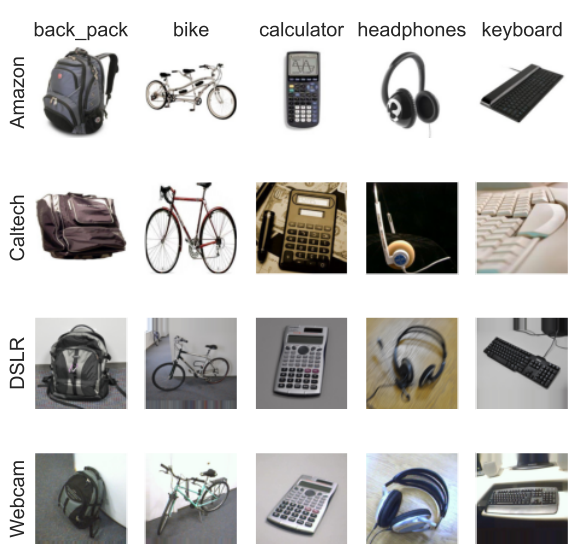
B.3. Training Details

Local learning rate and optimizer. For ResNet-18, the local learning rate (LR) $\eta = 0.1$, and for six-layer CNN and four-layer CNN, $\eta = 0.01$. For Office-Caltech-10, Digits-Five, and CIFAR-100, we use SGD optimizer with momentum 0.9. For DomainNet, we use SGD optimizer with momentum 0.9 and weight decay 1×10^{-4} .

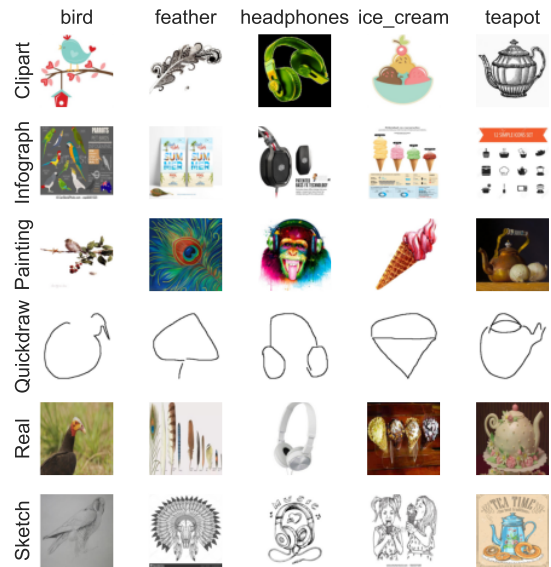
Local epochs E and communication rounds T . If not mentioned otherwise, we use the following settings of E and T . For Office-Caltech-10, we set local epochs $E = 5$, communication rounds $T = 120$. For DomainNet with the number of clients $N = 6$, we set local epochs $E = 5$, communication rounds $T = 200$. For Digits-Five, we set local epochs $E = 1$, communication rounds $T = 50$. For CIFAR-100 with $N \in \{5, 10, 15\}$, we set local epochs $E = 2$, communication rounds $T = 100$. For CIFAR-100 with $N = 20$, we set local epochs $E = 5$, communication rounds $T = 100$.

Hyperparameters. For our FediOS, we set $\lambda_{\text{FediOS}} = 0.1$ in Office-Caltech-10, DomainNet and CIFAR-100, and $\lambda_{\text{FediOS}} = 0.0$ in Digits-Five. In this paper, we keep $\alpha_{\text{FediOS}} = 0.5$ in all datasets and settings. We set $\alpha_{\text{FedDyn}} = 0.1$ for ResNet-18 and $\alpha_{\text{FedDyn}} = 0.01$ for six-layer CNN and four-layer CNN as suggested in their official implementations or papers. For MOON, we set $\mu_{\text{MOON}} = 1.0$ and $\tau_{\text{MOON}} = 0.5$. For Ditto, the learning setting of the personalized model is the same as the one of the global model. For FedProto, we set $\lambda_{\text{FedProto}} = 1.0$ as suggested in the paper [39]. We set $\lambda_{\text{FedCP}} = 0.1$ for ResNet-18 and six-layer CNN, and $\lambda_{\text{FedCP}} = 5.0$ for four-layer CNN. For pFedVEM, we train the feature extractor and classifier head of the network with the same learning rate and number of training

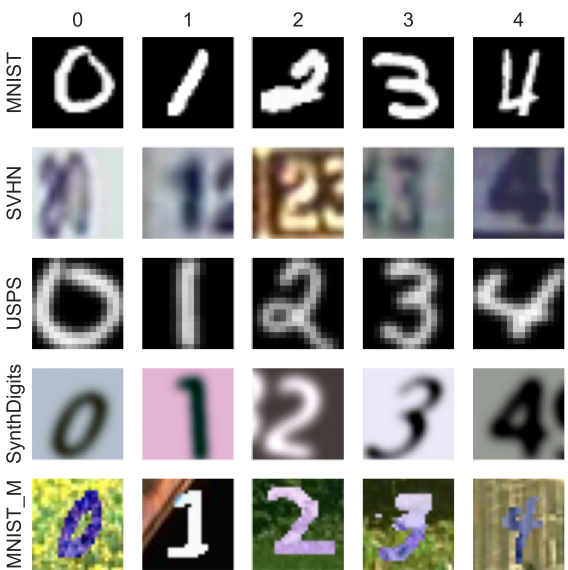
epochs, and MC sampling is fixed to 5 times as suggested in the paper [51].



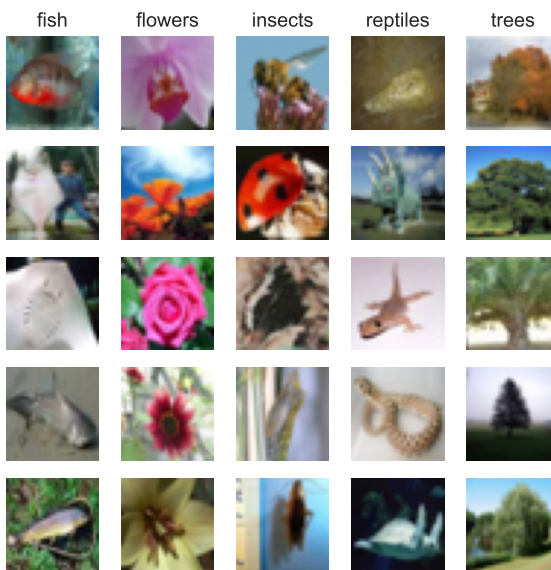
(a) Office-Caltech-10.



(b) DomainNet.



(c) Digits-Five.



(d) CIFAR-100.

Figure 6. **Demonstration of case samples from four datasets.** For each dataset, we selected five classes for illustration.